J. Chem. Sci. Vol. 128, No. 4, April 2016, pp. 501–509. © Indian Academy of Sciences.
DOI 10.1007/s12039-016-1053-9

Crystal structures of *meso*-tetrakis(2′,6′/3′,5′-difluorophenyl)porphyrins and their metal complexes: Influence of position of the fluoro groups on their structural properties

BHYRAPPA PUTTAIAH* and KARUPPAIAH KARUNANITHI
Department of Chemistry, Indian Institute of Technology Madras, Chennai 600036, India
e-mail: byra@iitm.ac.in

MS received 18 December 2015; revised 22 January 2016; accepted 27 January 2016

Abstract. Two series of non-solvated structures of 5,10,15,20-tetrakis(2′,6′/3′,5′-difluorophenyl)porphyrins, H_2T(2′,6′/3′,5′-DFP)P and their metal (Cu(II) and Zn(II)) complexes were determined by single crystal XRD. H_2(2′,6′-DFP)P, **1** and its metal (Cu(II), **2** and Zn(II), **3**) complexes showed near planar geometry of the porphyrin ring with the maximum root-mean-square (r.m.s.) which is the average deviation of the 24 core atoms from their least-squares plane by 0.056(3) Å while MT(3′,5′-DFP)P (Cu(II), **4** and Zn(II), **5**) structures feature significant distortion of the macrocycle (r.m.s. = 0.22(2) Å). Nearly planar structures **1-3** revealed more number of intermolecular short contacts than that observed in nonplanar structures **4** and **5**. Normal coordinate structure decomposition analysis of the structures **1**-**3** revealed negligible *wave* distortion of the macrocycle but the corresponding nonplanar **4** and **5** structures feature mainly *ruffled* combined with minimal *saddled* distortions. The increased nonplanarity of the less sterically hindered derivatives **4** and **5** has been ascribed to intermolecular interactions and/or crystal packing forces.

Keywords. substituted porphyrins; fluorinated porphyrins; *meso*-tetraarylporphyrins; crystal structures; NSD analysis.

1. Introduction

Synthetic analogues of naturally occurring tetrapyrroles are of remarkable interest due to their ease of synthesis, facile functionalization and capable of incorporating variety of metal ions to its four nitrogen core.[1–3] Such systems have been widely used in potential applications such as molecular sieves,[4,5] catalysis,[6–14] sensors[15–21] and dye sensitized solar cells.[22–24] Introduction of substituents at the periphery of the macrocycle and core metal ions alters the electronic properties of the porphyrin π-system. The use of synthetic analogues showed that the core metal ion and the peripheral substituents influence the stereochemistry of the porphyrin macrocycle.[25,26] Distortion of the macrocycle in various hemeproteins has been examined by normal-coordinate structure decomposition analysis.[27] Introduction of β-substituents at the periphery of the *meso*-tetraphenylporphyrin, TPP produces unique physicochemical properties including variable nonplanar distortion of the macrocycle[1,28] and such distortions arise owing to steric repulsive interactions among the peripheral substituents.[29,30]

Numerous crystal structure reports are available on variety of porphyrins and metalloporphyrins.[31–38] Systematic analyses of the change in conformation of the macrocycle as a function of the core metal ion and the substituents have been well-documented in the literature.[28] The MTPPs are known to form porphyrin sponges with varying degree of lattice solvates.[39,40] Alternatively, introduction of mixed substituents on all the β-pyrrole positions of MTPPs revealed varying degree of nonplanarity of the porphyrin ring.[41–43]

Earlier report on β-octafluoro-*meso*-tetrakis(pentafluorophenyl)porphinato zinc(II) complexes revealed moderate distortion of the porphyrin ring induced by the steric crowding of the peripheral substituents.[44,45] In the case of metal ion coordination networks, the position of the nitrogen atoms at the *meso*-pyridyl or *meso*-carboxy phenyl groups produced interesting three-dimensional packing motifs with varying lattice solvates.[4,46–48] Some of these network solids are stable even at elevated temperatures and showed selective recognition of guest molecules.[5,49,50] Interestingly, *meso*-tetrakis(2′,6′-dihydroxyphenyl)porphyrin and *meso*-tetrakis(3′,5′-dihydroxy phenyl)porphyrin exhibited hydrogen bonded networks with ethyl acetate as the lattice solvates.[51] An earlier report on free base 5,10,15,20-tetrakis(3′, 5′-difluorophenyl)porphyrin showed moderate nonplanarity of the porphyrin ring.[52] Such distortions without steric crowding could explain the role of intermolecular interactions/

*For correspondence

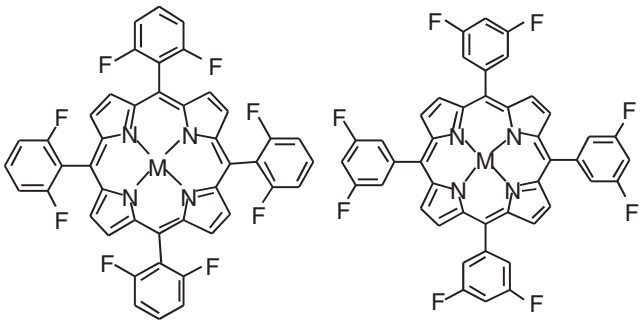

Figure 1. Chemical structures of fluorinated *meso*-tetraphenylporphyrins and their metal complexes.

crystal packing forces in the solid-state.[53–55] A recent report on the structure of 5,10,15-20-tetrakis(4-methoxyphenyl)porphinato copper(II) showed nonplanar distortion of the macrocycle and it was suggested to be due to C–H$\cdots\pi$ interactions.[53]

In an effort to examine the role of the position of the difluoro substituents at the di-*ortho* phenyl versus di-*meta* phenyl positions of the TPP, crystal structures of two series of lattice solvate free *meso*-tetrakis(2′, 6′/3′, 5′-difluorophenyl)porphyrin, H_2T(2′, 6′/3′, 5′-DFP)P and their metal (Zn(II) and Cu(II)) complexes (figure 1) have been determined which reveal interesting differences in their structural and molecular packing motifs.

2. Experimental section

2.1 *Materials*

H_2T(2′, 6′/3′, 5′-DFP)P[56,57] and their metal, Cu(II) and Zn(II) complexes were prepared using conventional procedures.[58] Synthesised porphyrins were characterised by electronic absorption, proton NMR and mass spectroscopic methods. All the solvents employed in this work are of analytical grade and used as received.

H_2T(2′,6′-DFP)P λ_{max}, nm (log ε): 413 (5.51), 508 (4.34), 536 (3.41), 585 (3.86), 638 (3.60). ^{1}H NMR in $CDCl_3$: 8.87 (s, 4H, $\beta-$pyrrole-H), 7.80 (m, 4H, *meso-p*-phenyl-H), 7.39 (t, 8H, *meso-m*-phenyl-H), –2.76 (s, 2H, NH). ESI-MS calculated for $C_{44}H_{22}N_4F_8$, (m/z): 759.0 (calcd., 758.66). **CuT(2′,6′-DFP)P**: λ_{max}, nm (log ε): 410 (5.40), 535 (4.15), 569 (3.69). MALDI-MS calculated for $C_{44}H_{20}N_4F_8Cu$, (m/z): 819.39 (Cacld., 819.08). **ZnT(2′, 6′-DFP)P**: λ_{max}, nm (log ε): 415 (5.58), 544 (4.28), 578 (sh). ^{1}H NMR in $CDCl_3$: 8.96 (s, 8H, $\beta-$pyrrole-H), 7.80 (m, 4H, *meso-p*-phenyl-H), 7.38 (t, 8H, *meso-m*-phenyl-H). MALDI-MS calculated for $C_{44}H_{20}N_4F_8Zn$, (m/z): 820.42 (Cacld., 820.08). **H_2T(3′,5′-DFP)P**: λ_{max}, nm (log ε): 416 (5.40), 511 (4.14), 545 (3.58), 587 (3.66), 644 (3.27). ^{1}H NMR in $CDCl_3$: 8.89 (s, 8H, $\beta-$pyrrole-H), 7.76 (m, 8H, *meso-o*-phenyl-H), 7.31 (t, 4H, *meso-p*-phenyl-H), –2.96 (s, 2H, NH). ESI-MS calcd for $C_{44}H_{22}N_4F_8$ (m/z): 759 (calcd., 758.66). **CuT(3′,5′-DFP)P**: λ_{max}, nm (log ε): 412 (5.45), 537 (4.18), 568 (sh). MALDI-MS calcd for $C_{44}H_{20}N_4F_8Cu$, (m/z): 819.42 (Cacld., 819.08). **ZnT(3′, 5′-DFP)P**: λ_{max}, nm (log ε): 417 (5.45), 546 (4.12), 578 (sh). ^{1}H NMR in $CDCl_3$: 8.99 (s, 8H, $\beta-$pyrrole-H), 7.76 (d, 8H, *meso-o*-phenyl-H), 7.32 (t, 4H, *meso-p*-phenyl-H). MALDI-MS calculated for $C_{44}H_{20}N_4F_8Zn$, (m/z): 820.44 (Cacld., 820.08).

2.2 *Instrumentation*

Electronic absorption spectra of porphyrins were recorded on a JASCO V-550 model absorption spectrophotometer using a pair of matched quartz cells of 10 mm path length at 298 K. ^{1}H NMR spectra of fluorinated pophyrins were measured on a Avance 400 MHz NMR spectrometer using $CDCl_3$ as the solvent with tetramethylsilane as the internal reference at ambient temperature. Mass spectral measurements of the samples were carried out with electrospray ionization (ESI) mass spectrometer model Micromass Q-TOF Micro using 10% formic acid in methanol as the solvent medium. A matrix assisted laser desorption ionisation time-of-flight (MALDI-TOF) spectrum on a Voyager DE-PRO model mass spectrometer was used by employing α-cyano-4-hydroxycinnamic acid as the matrix.

2.3 *Crystal structures*

Crystals of MT(2′, 6′-DFP)P (2H, Cu(II) and Zn(II)), **1-3** and MT(3′, 5′-DFP)P (M = Cu(II), Zn(II)) (**4** and**5**) complexes were grown by diffusing vapors of *n*-hexane to the saturated solution of porphyrin in chloroform solution over a period of five days. Single crystal X-ray structure data collections were performed on a Bruker AXS Kappa Apex II CCD diffractometer equipped with graphite monochromated Mo K_α radiation (λ = 0.71073 Å). The crystals were coated with inert oil, mounted on a glass capillary, transferred to the cold nitrogen gas stream of the diffractometer and crystal data was collected at 173 K. The reflections with $I > 2\sigma(I)$ were employed for structure solution and refinement. The SIR92[59] (WINGX32) program was used for solving the structure by direct methods. Successive Fourier synthesis was employed to complete the structures after full matrix least-squares refinement on $|F|^2$

Table 1. Crystallographic data of fluorinated porphyrins, **1**, H_2T(2′, 6′-DFP)P; **2**, CuT(2′, 6′-DFP)P; **3**, ZnT(2′, 6′-DFP)P; **4**, CuT(3′, 5′-DFP)P; **5**, ZnT(3′, 5′-DFP)P.

	1	**2**	**3**	**4**	**5**
Empirical formula	$C_{44}H_{22}F_8N_4$	$CuC_{44}H_{20}F_8N_4$	$ZnC_{44}H_{20}F_8N_4$	$CuC_{44}H_{20}F_8N_4$	$ZnC_{44}H_{20}F_8N_4$
Formula weight	758.66	820.18	822.01	820.18	822.01
color	pink	pink	purple	purple	pink
crystal system	monoclinic	monoclinic	monoclinic	tetragonal	tetragonal
Space group	$P2_1/c$	$P2_1/c$	$P2_1/c$	I -4 2d	I -4 2d
a (Å)	12.4747(7)	12.4838(7)	12.4783(4)	15.443(2)	15.477(3)
b (Å)	11.3662(5)	11.3498(6)	11.3775(3)	15.443(2)	15.477(3)
c (Å)	12.1184(7)	12.0971(5)	12.1077(3)	14.045(3)	14.002(3)
α(°)	90	90	90	90	90
β(°)	96.934(2)	96.514(3)	96.6620(10)	90	90
γ(°)	90	90	90	90	90
vol (Å^3)	1705.70(16)	1702.96(15)	1707.35(8)	3349.3(11)	3354.0(12)
Z	2	2	2	4	4
d_{calc}(mg/m^3)	1.477	1.600	1.599	1.627	1.628
Wavelength λ, Å	0.71073	0.71073	0.71073	0.71073	0.71073
T(K)	173(2)	173(2)	173(2)	173(2)	173(2)
No. of unique reflections	3029	2916	2961	2088	2079
no. of parameters refined	254	259	259	130	129
GOF on F^2	1.039	1.029	1.090	1.084	1.037
R_1^a	0.0516	0.0484	0.0407	0.0236	0.0334
wR_2^b	0.1219	0.1065	0.1334	0.0619	0.0861

[a]$R_1 = \sum \|F_o| - -|F_c\|/\sum |F_o|$; $I_o > 2\sigma(I_o)$. [b]$wR_2 = [\sum w(F_o^2 - F_c^2)^2/\sum w(F_o^2)^2]^{1/2}$.

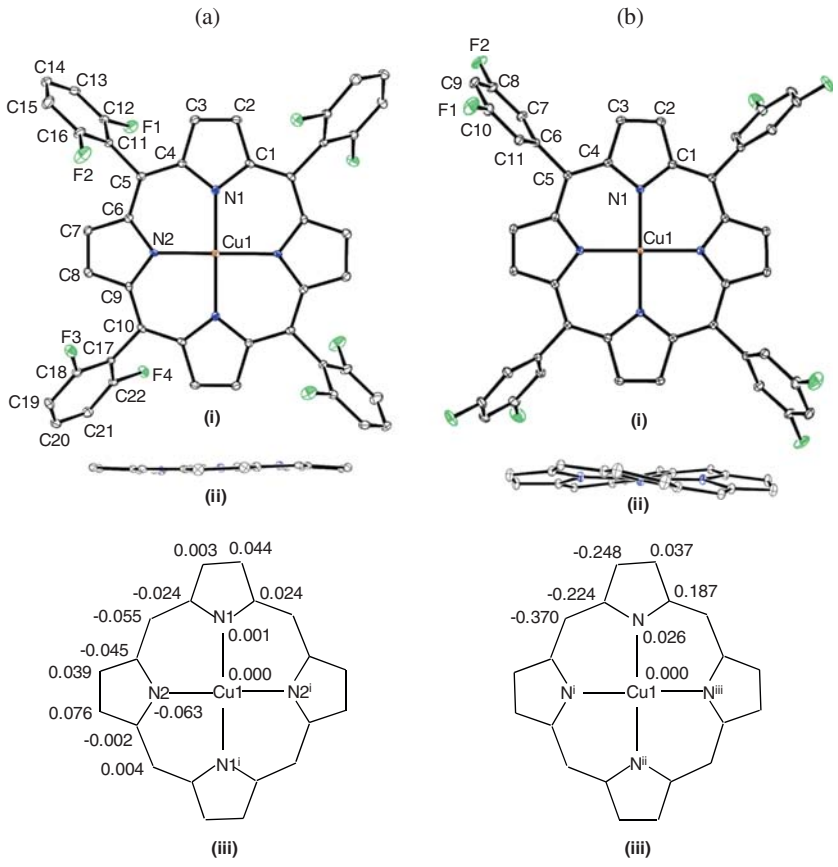

Figure 2. ORTEP drawings for structures **2**[**a**(i), **a** (ii)] and **4**[**b**(i), **b**(ii)] (thermal ellipsoids shown at 30% probability level). The mean plane displacement of the 24-atom macrocycle in Å (esd's < 0.003 Å) units for **2** and **4** are given in (**a**)(iii) and (**b**)(iii), respectively.

using SHELXL97 software.[60] Fourier syntheses led to the location of all the non-hydrogen atoms. For the structure refinement, all data were used including negative intensities. Non-hydrogen atoms were refined with anisotropic thermal parameters. All the hydrogen atoms in the porphyrin structure could be located in the difference map. However, the hydrogen atoms were geometrically relocated at chemically meaningful positions and were given riding model refinement. ORTEP drawings of the structures were drawn using ORTEP3[61] program. Molecular packing diagrams and intermolecular short contacts of the fluorinated porphyrins were generated using Mercury 3.5[62] programs.

Crystallographic information files of the structures with the CCDC numbers, $H_2T(2',6'\text{-DFP})P$, **1** (920338) and $CuT(2',6'\text{-DFP})P$, **2** (920339), $ZnT(2',6'\text{-DFP})P$, **3** (920340), $CuT(3',5'\text{-DFP})P$, **4** (920341) and $ZnT(3',5'\text{-DFP})P$, **5** (920342) have been submitted to the Cambridge Crystallographic Data Centre as the supplementary material.

3. Results and Discussion

Electronic absorption spectra of $H_2T(2',6'\text{-DFP})P$, **1** and $H_2T(3',5'\text{-DFP})P$ feature an intense Soret, B and four visible 'Q' transitions. Compound **1** exhibited blue-shifted absorption when compared to $H_2T(3',5'\text{-DFP})P$. Their metal complexes, $CuT(2',6'\text{-DFP})P$, **2** and $ZnT(2',6'\text{-DFP})P$, **3** exhibited a 'B' and two visible bands with marginal blue shifted absorption bands in contrast to compounds $CuT(3',5'\text{-DFP})P$, **4** and $ZnT(3',5'\text{-DFP})P$, **5**. Copper(II) complexes (**2** and **4**) featured slightly blue-shifted absorption when compared to their corresponding Zn(II) complexes (**3** and **5**). This is perhaps due to stabilisation of highest occupied π-molecular orbital, HOMO, a_{2u} relative to a_{1u}, since a_{2u} orbital has electron density contribution from the imino nitrogens and *meso*-carbons.[63] The observed spectral pattern and intensity of the bands are similar to the reported data of the corresponding MTPPs.[63] The red-shift of the electronic absorption bands of **4**

Table 2. Selected mean bond lengths, angles and geometrical parameters of fluoroporphyrins.

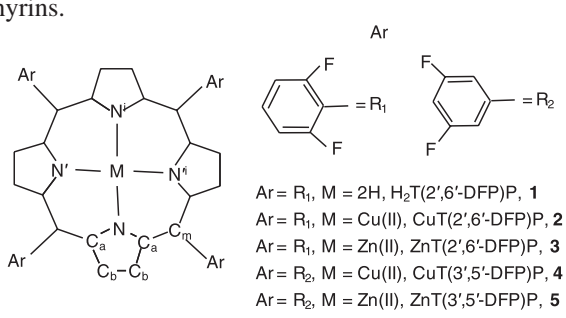

	1	2	3	4	5
Distance (Å)					
M–N		2.002(3)	2.039(2)	1.995(1)	2.028(2)
C_a–N	1.366(3)	1.380(4)	1.377(4)	1.374(2)	1.371(3)
C_a–C_b	1.440(4)	1.435(5)	1.443(4)	1.443(2)	1.442(3)
C_b–C_b	1.348(4)	1.345(5)	1.352(4)	1.359(2)	1.358(3)
C_a–C_m	1.399(4)	1.390(5)	1.396(4)	1.401(2)	1.405(3)
Angle (°)					
$(N–M–N)_{adj}$	–	90.0(1)	90.0(1)	90.0(1)	90.0(1)
$(N–M–N)_{opp}$	–	180.0	180.0	178.5(1)	177.7(1)
M–N–C_a	–	127.3(2)	126.6(2)	127.0(1)	126.6(2)
C_a–N–C_a	107.9(2)	105.4(3)	106.5(2)	105.9(1)	106.6(2)
C_a–C_m–C_a	126.1(3)	124.6(3)	125.8(3)	123.5(1)	124.9(2)
N–C_a–C_m	125.9(2)	125.4(3)	125.4(2)	125.5(1)	125.3(2)
C_b–C_a–C_m	125.4(2)	124.6(3)	125.1(3)	124.2(1)	125.0(2)
C_a-C_m-C_a-N	3.6(2)	2.2(6)	2.6(3)	6.9(3)	6.9(4)
Geometrical parameters (Å)					
ΔM^a (Å)	–	0.000(1)	0.040(1)	0.000	0.000
r.m.s. (Å)	0.056(2)	0.039(3)	0.040(2)	0.218(2)	0.199(2)
N....N^i	4.076	3.998	4.065	3.989	4.055
N′....N'^i	4.188	4.007	4.090	–	–
meso-Ph^b	70.1(1)°	71.4(2)°	71.2(1)°	72.8(1)°	72.5(1)°
$pyrrole^b$	3.5(1)°	2.5(2)°	2.7(1)°	11.7(1)°	10.7(1)°

[a]displacement of the metal ion from 24-atom core.
[b]dihedral angle relative to 24-atom core.

and **5** is perhaps influenced by the nonplanarity of the macrocycle.[29] ^{1}H NMR spectra of **1**, **3** and **5** compounds exhibited resonances arising from *meso*-aryl and β-pyrrole protons while compound **1** showed additional imino-proton resonances. The observed resonances are not significantly different from those reported for the unsubstituted H_2TPP.[64] The integrated intensity of the proton resonances is consistent with the expected number of protons present in the proposed structures.

The structures **1-3** are isomorphous and crystallise in monoclinic, $P2_1/c$ system with $Z = 2$ and show half the molecule in the asymmetric unit. Structures **4** and **5** are also isomorphous with tetragonal I-4 2d with $Z = 4$ and shows quarter of a molecule in the asymmetric unit. These two structures are isomorphous with the reported H_2T(3′, 5′-DFP)P structure. Crystallographic data for all the structures (**1-5**) are listed in (table 1). Representative ORTEP drawings and mean plane displacement of 24-atom core of the Cu(II)-complex structures (**2** and **4**) are shown in figure 2. The selected mean bond lengths, angles and geometrical parameters of the macrocycle for all the structures **1-5** are listed in table 2. Structure **1** features similar bond lengths and angles to that of the reported H_2T(3′, 5′-DFP)P[52] and H_2TPP.[65] Further, observed MN_4 core of the porphyrins **1** and **2** are comparable to the reported room temperature crystal structures of MT(2′, 6′-DFP)P (M = 2H and Cu(II)).[66] The imnio nitrogens bearing protons feature shorter C_a–N–C_a (105.2(2)°) relative to C_a–N'–C_a (110.5(2)°) angle. Similar trend in angles were reported for H_2T(3′, 5′-DFP)P. As anticipated, the mean (Cu–N)[67–69] is slightly shorter than $(Zn–N)_{av}$[70–73] bond lengths and are similar to the reported corresponding MTPPs.

The displacement of the core atoms from the 24-atom core indicates significant distortion of the porphyrin ring in **4** relative to **2** (figure 2). The representative plot for linear displacement of 24-atom core of the complexes, **2** and **4** is shown in figure 3. Both **4** and **5** structures feature nonplanar distortion of the porphyrin ring as evidenced from slight increase in average C_a–C_m bond length and decrease in C_a–C_m–C_a angle as well as an increase in C_a–C_m–C_a–N torsion angle relative to the corresponding structures **2** and **3**. The extent of displacement (rms <0.056 Å) of the 24-atom core in **1-3** structures suggests minimal *wave* distortions while the **4** and **5** have significant distortions (rms <0.218 Å) mainly *ruffled* with less contribution from *saddled* distortion. It can be seen that the side views of **2** and **3** show near planarity of the porphyrin ring (figure 3). The macrocycle in **2** and **3** are more planar in comparison to their parent free base structure, **1** and this may be due to the presence of core metal ions. The average N...N

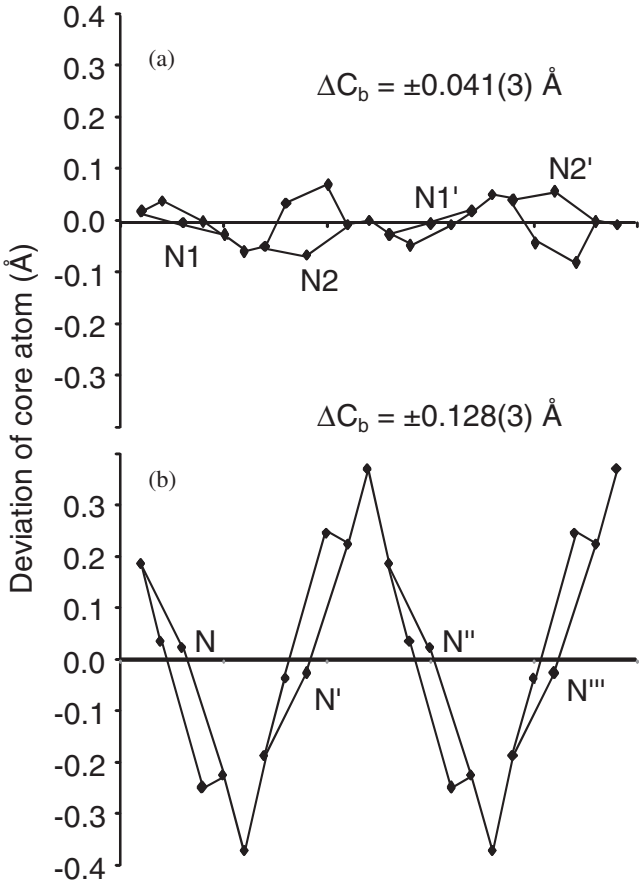

Figure 3. Depicts the linear displacement of 24-atom core of **(a)** for **2** and **(b)**, for **4** structure, respectively.

separation in the structures **1-5** (table 2) indicates contraction of the MN_4 core relative to N_4H_2 core and follows the order: **1** (4.132 Å) > **5** (4.055 Å) > **3** (4.078 Å) > **2** (4.003 Å) > **4** (3.989 Å). The increase in nonplanar distortion for **4** and **5** is evident from the increase in dihedral angles of the pyrrole groups relative to the planar structures **1-3** (table 2). The crystal structure report of FeT(2′,6′-DFP)P(OCH_3) showed slight distortion of the porphyrin ring.[73]

The molecular packing diagrams for the structures **1-5** have been examined to probe the role of intermolecular interactions on the stereochemistry of the porphyrin ring. In **1**−**3**, the molecules are arranged in a zigzag fashion with an angle of 64° relative to 24-atom core mean planes (figure 4), whereas **4** and **5** showed analogous molecular packing in the crystals, where they are aligned in a slip-stacked fashion (figure 5). However, the porphyrin structures **1**−**5** show negligible $\pi \cdots \pi$ stacking interactions. Their shortened inter-porphyrin contacts are listed in table 3. It is of interest to note that both free base porphyrin and its metal complexes exhibit similar packing features.

The molecular packing diagram of **2** is depicted in figure 4. The shortest distance between the mean planes of the 24-atom core of the two adjacent porphyrins which are parallel to each other are separated by 15.32 Å. The closest distance between the Cu···Cu centres in **2** for the two adjacent porphyrins oriented parallel

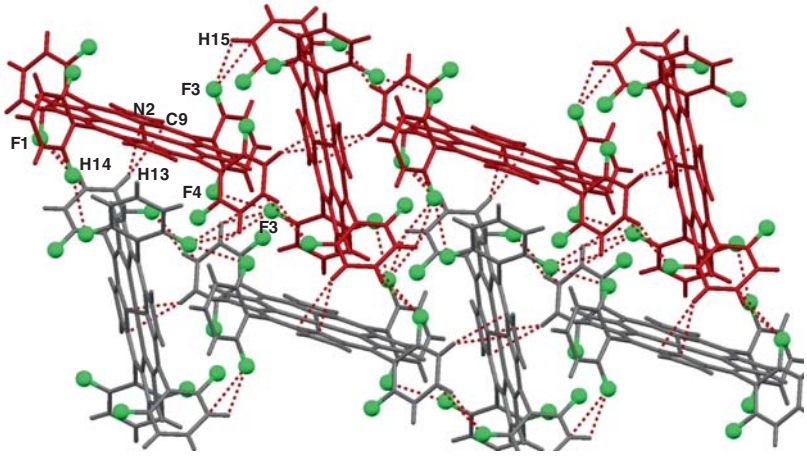

Figure 4. Molecular packing motif showing two dimensional layer structure for **2** (layer oriented perpendicular to unit cell 'bc' plane). The interconnected zigzag one-dimensional chains are shown in two different colours and fluorine atoms in green ball stick model. Dotted red lines denote the intermolecular short contacts.

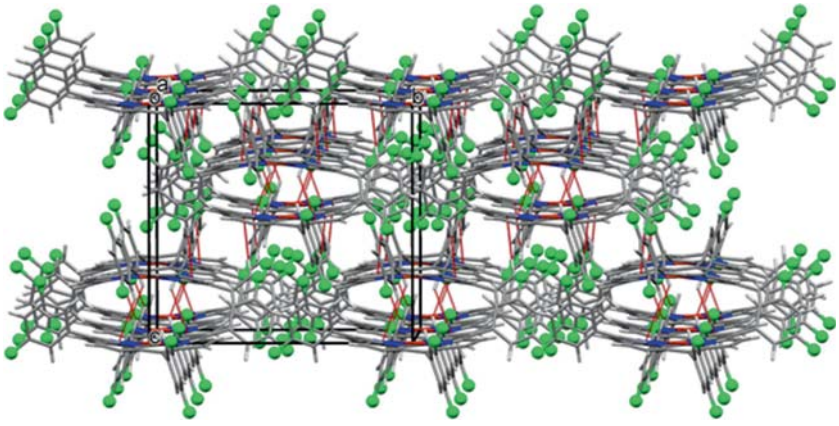

Figure 5. The molecular packing diagram of **4** viewed approximately down 'a' axis. The C−H···π contacts are indicated in dotted red lines. Color scheme: C, dark grey, H, light grey, N, blue and Cu, red and F, green spheres.

Table 3. Intermolecular short contact distances (in Å) for structures **1**-**5**.

Short contacts	**1**	**2**	**3**	**4**	**5**
C−F···H$_{(ph)}$	2.51−2.63 (2.499−2.652)[a]	2.46−2.63 (2.471−2.636)[a]	2.48−2.63	–	–
C−F···C$_{\pi(ph)}$	3.082−3.138 (3.091)[a]	3.045−3.142 (3.063, 3.165)[a]	3.061−3.133	–	–
F···F	2.909	2.933	2.929	–	–
$_{(pyr/ph)}$C−H···C$_{\pi(pyr/ph)}$	2.73, 2.89 (2.760)[a]	2.74	2.74	2.89	2.86
$_{(ph)}$C−H···N	2.73 (2.741)[a]	2.74	2.72	–	–

[a]The data given in parentheses are taken from ref. [66].

Table 4. Normal-coordinate structure decomposition analysis of fluorinated porphyrins.

	D_{oop}	B_{2u},*sad*	B_{1u},*ruf*	A_{2u},*dom*	$E_g(x)$,*wav(x)*	$E_g(y)$,*wav(y)*	A_{1u},*prop*	sum	*sad*/ sum (%)	*ruf*/ sum (%)	*dom* / sum (%)
Out-of-plane displacements (Å)											
1[a]	0.2600	−0.0001	−0.0001	0.0000	0.2390	−0.1024	−0.0001	0.3417	0	0	0
2[a]	0.1866	0.0000	0.0006	−0.0002	0.0810	0.1681	0.0002	0.2501	0	∼0	∼0
3[a]	0.2089	0.0000	0.0001	0.0001	−0.1978	0.0672	−0.0001	0.2653	∼0	∼0	∼0
4	1.0639	−0.2837	−1.0254	0.0000	−0.0000	0.0000	0.0000	1.3091	21.67	78.32	0
5	0.9631	0.2490	0.9303	0.0000	0.0000	0.0000	0.0000	1.1793	21.11	78.88	0
6	0.9908	0.2936	0.9463	0.0008	0.0000	0.0000	0.0004	1.2411	23.65	76.25	∼0
In-plane displacements (Å)											
	D_{ip}	B_{2g}, *m-str*	B_{1g}, *N-str*	$E_u(x)$, *trn(x)*	$E_u(y)$, *trn(y)*	A_{1g}, *bre*	A_{2g}, *rot*	*sum*	B_{2g}/*sum*,%	B_{1g} / sum, %	A_{1g} / sum, %
1	0.2004	0.0098	−0.0025	0.0001	0.0000	0.2000	0.0071	0.2195	4.46	1.13	91.12
2	0.0355	0.0091	−0.0109	0.0003	0.0004	0.0326	0.0013	0.0546	16.67	19.96	59.71
3	0.3967	0.2331	−0.2868	0.0000	0.0002	0.1443	0.0004	0.6648	35.1	43.15	21.7
4	0.0432	0.0000	0.0000	0.0000	0.0000	−0.0341	0.0265	0.0606	0	0	56.27
5	0.0853	0.0000	0.0000	0.0000	0.0000	0.0803	0.0289	0.1092	0	0	73.53
6	0.0983	0.0000	0.0000	0.0000	0.0000	0.0920	0.0348	0.1268	0	0	72.55

6, H_2T(3',5'-DFP)P; [a]Mainly *wav(x), wav(y)* distortions.

and nearly orthogonal to each other in the one-dimensional zigzag chains are 16.59 Å and 8.29 Å, respectively. These one-dimensional arrays form a layer-like structure, which is approximately parallel to 'bc' plane of the unit cell. The inter-porphyrin interactions within the layer are dominated by $_{(ph)}C-H\cdots C_{\pi(pyr)}$, $_{(ph)}C-H\cdots N_{\pi(pyr)}$ and $C-F\cdots H_{(ph)}$ close contacts (table 3). These layers are interacting *via* $C-F\cdots C_{(ph)}$, $C-F\cdots H_{(ph)}$ and $F\cdots F$ short contacts to form a three dimensional packing motif (figure 4).

The molecular packing diagram of **4** is depicted in figure 5. This may be visualised as the slip-stacked arrangement of porphyrins to form one-dimensional array and they are oriented parallel to the unit cell 'a' axis. The porphyrin ring mean planes of the offset molecules are separated by 3.511 Å. Similar crystal packing is also observed in **5**. It can be seen from table 3, that the structures **4** and **5** have less intermolecular short contacts than **1-3**. The two non-interacting one-dimensional molecular arrays in **4** and **5** are sandwiched between one array from above and another array from below *via* $_{(ph)}C-H\cdots C_{\pi(pyr)}$ interactions (figure 5) with longer short contact distances relative to that in the corresponding structures **2** and **3** (table 3). The distortion of the porphyrin ring in **4** and **5** is similar to that reported in their parent H_2T(3′,5′-DFP)P and it is perhaps due to crystal packing forces and/or intermolecular interactions.[53–55] The short contact distances observed in these structures indicates existence of weak intermolecular interactions.[74–76] The structures **1** and **2** showed similar molecular packing diagram to that of their corresponding structures[66] reported at 298 K. Generally, the low temperature structures (**1** and **2**) examined in this study revealed more number of other types of inter-porphyrin short contact distances than the reported structures at 298 K (table 3).

4. Normal-coordinate structure decomposition analysis

Normal coordinate structural decomposition analysis of the these fluorinated porphyrins were carried out using reported method.[77] The out-of-plane displacement values (D_{oop}) based on the minimum basis set for the macrocyclic ring atoms indicate negligible distortion of the porphyrin ring in **1-3** relative to H_2T(3′,5′-DFP)P and **4-5** complexes (table 4). The sum values are from all the distortions calculated by ignoring the signs on the individual distortion values. The structures **1-3** feature mainly *wav (x)* and *wav (y)* distortions while the **4** and **5** revealed mainly *ruf* (∼75-78%) combined with *sad* (21-24%) distortions. Generally, in-plane-

displacement of the core atoms indicate higher D_{ip} values for **1-3** in contrast to that observed for the corresponding **4** and **5** structures. In case of **1-3** structures, *m-str*, *N-str*, *bre* and *rot* distortions are predominant while it is mainly *bre* and *rot* distortions in H_2T(3′,5′-DFP)P, **4** and **5**. Such a trend is anticipated due to the distortion of the core atoms in the coplanar rings.[78] The observed out-of-plane distortions are consistent with the type of displacements revealed in their respective crystal structures.

5. Conclusions

The structures of two series of fluorinated porphyrins, MT(2′, 6′/3′, 5′-DFP)P (M = 2H, Cu(II) and Zn(II)) have been examined by single crystal XRD analysis. Upon changing the substituents from di-*ortho* to di-*meta*-phenyl positions, a marked change in distortion of the porphyrin rings were observed. Macrocycle in structures **1-3** are nearly planar with pronounced intermolecular short contacts but structures **4** and **5** revealed significant distortion with negligible intermolecular contacts. This suggests the positional influence of the fluorine atoms in structures **4** and **5** including the crystal packing forces and intermolecular short contacts on the nonplanarity of the macrocycle. Normal-coordinate structure decomposition analysis of structures revealed very negligible out-of-plane *wave* distortions in **1-3** while **4** and **5** showed mainly *ruffling* combined with minimal *saddling* of the macrocycle.

Acknowledgements

This work was supported financially from the project grant (SR/S1/IC-2007) Department of Science and Technology (DST), Govt. of India to Dr. PB. We thank Mr. V. Ramkumar for XRD data collection and department of chemistry (IIT Madras) for single crystal XRD facility.

References

1. Kadish K M, Smith K M and Guilard R (Eds.) 2000–2013 In *Handbook of Porphyrin Science* Vol. 1–25 (London: World Scientific)
2. Kadish K M, Smith K M and Guilard R 2000 In *The Porphyrin Handbook* Vol. 1-10 (San Diego: Academic Press)
3. Lindsey J S 2010 *Acc. Chem. Res.* **43** 300
4. Suslick K S, Bhyrappa P, Chou J H, Kosal M E, Nakagaki S, Smithenry D W and Wilson S R 2005 *Acc. Chem. Res.* **38** 283
5. Kosal M E, Chou J H, Wilson S R and Suslick K S 2002 *Nature Mater.* **1** 118
6. Dolphin D, Traylor T G and Xie L Y 1997 *Acc. Chem. Res.* **30** 251
7. Traylor T G and Tsuchiya S 1987 *Inorg. Chem.* **26** 1338
8. Hoffmann P, Labat G, Robert A and Meunier B 1990 *Tetrahedron Lett.* **31** 1991
9. Costentin C, Robert M and Seavant J M 2015 *Acc. Chem. Res.* **48** 2996
10. Wu Z S, Chen L, Liu J, Parvez K, Liang H, Shu J, Sachdev H, Graf R, Feng X and Müllen K 2014 *Adv. Mater.* **26** 1450
11. Lin S, Diercks C, Zhang Y B, Kornienko N, Nichols E M, Zhao Y, Paris A R, Kim D, Yang P, Yaghi O M and Chang C J 2015 *Science* **349** 1208
12. Grinstaff M W, Hill M G, Labinger L A and Gray H B 1994 *Science* **264** 1311
13. Meunier B 1992 *Chem. Rev.* **92** 1411
14. Hod I, Sampson M D, Deria P, Kubiak C P, Farha O K and Hupp J T 2015 *ACS Catal.* **5** 6302
15. Tu W, Lei J, Jian G, Hu Z and Ju H 2010 *Chem. Eur. J.* **16** 4120
16. Kang Y, Kampf J W and Meyerhoff M E 2007 *Anal. Chim. Acta* **598** 295
17. Filippini D, Alimelli A, Di Natale C, Paolesse R, D'Amico A and Lundstroem I 2006 *Angew. Chem. Int. Ed.* **45** 3800
18. Badr I H A and Meyerhoff M E 2005 *J. Am. Chem. Soc.* **127** 5318
19. Buehlmann P, Pretsch E and Bakker E 1998 *Chem. Rev.* **98** 1593
20. Zhou X, Lee S, Xu Z and Yoon J 2015 *Chem. Rev.* **115** 7944
21. Askim J R, Mahmoudi M and Suslick K S 2013 *Chem. Soc. Rev.* **42** 8649
22. Panda M K, Ladomenou K and Coutsolelos A G 2012 *Coord. Chem. Rev.* **256** 2601
23. Li L L and Diau E W G 2013 *Chem. Soc. Rev.* **42** 291
24. Urbani M, Grätzel M, Nazeeruddin K M and Torres T 2014 *Chem. Rev.* **114** 12330
25. Scheidt W R 2000 In *The Porphyrin Handbook* Kadish K M, Smith K M and Guilard R (Eds.) (San Diego: Academic Press) Vol. 3 p. 49
26. Scheidt W R and Lee Y J 1987 *Struct. Bonding (Berlin)* **64** 1
27. Shelnutt J A 2000 In *The Porphyrin Handbook* Kadish K M, Smith K M and Guilard R (Eds.) (San Diego: Academic Press) Vol. 7 p. 167
28. Senge M O 2000 In *The Porphyrin Handbook* Kadish K M, Smith K M and Guilard R (Eds.) (San Diego: Academic Press) Vol. 1 p. 239
29. Shelnutt J A, Song X Z, Ma J G, Jia S L, Jentzen W and Medforth C J 1998 *Chem. Soc. Rev.* **27** 31
30. Ravikanth M and Chandrashekar T K 1995 *Struct. Bonding (Berlin)* **82** 107
31. Renner M W, Barkigia K M, Zhang Y, Medforth C J, Smith K M and Fajer J 1994 *J. Am. Chem. Soc.* **116** 8582
32. Sparks L D, Medforth C J, Park M S, Chamberlain J R, Ondrias M R, Senge M O, Smith K M and Shelnutt J A 1993 *J. Am. Chem. Soc.* **115** 581
33. Barkigia K M, Renner M W, Furenlid L R, Medforth C J, Smith K M and Fajer J 1993 *J. Am. Chem. Soc.* **115** 3627
34. Panda P K and Krishnan V 2005 *J. Chem. Sci.* **115** 73
35. Regev A, Galili T, Medforth C J, Smith K M, Barkigia K M, Fajer J and Levanon H 1994 *J. Phys. Chem.* **98** 2550

36. Senge M O and Kalisch W W 1997 *Inorg. Chem.* **36** 6103
37. Barkigia K M, Berber M D, Fajer J, Medforth C J, Renner M W and Smith K M 1990 *J. Am. Chem. Soc.* **112** 8851
38. Senge M O 2000 In *The Porphyrin Handbook* Kadish K M, Smith K M and Guilard R (Eds.) (San Diego: Academic Press) Vol. 10
39. Byrn M P, Curtis C J, Hsiou Y, Khan S I, Sawin P A, Tendick S A, Terzis A and Strouse C E 1993 *J. Am. Chem. Soc.* **115** 9480
40. Byrn M P, Curtis C J, Khan S I, Sawin P A, Tsurumi R and Strouse C E 1990 *J. Am. Chem. Soc.* **112** 1865
41. Senge M O, Gerstung V, Senge K R, Runge S and Lehmann I 1998 *J. Chem. Soc., Dalton Trans.* 4187
42. Bhyrappa P, Arunkumar C and Varghese B 2009 *Inorg. Chem.* **48** 3954
43. Bhyrappa P, Sankar M and Varghese B 2009 *Inorg. Chem.* **45** 4136
44. Leroy J, Bondon A, Toupet L and Rolando C 1997 *Chem. Eur. J.* **3** 1890
45. Woller E K and DiMagno S G 1997 *J. Org. Chem.* **62** 1588
46. Goldberg I 2005 *Chem. Commun.* 1243
47. Lipstman S and Goldberg I 2010 *CrystEnggCommun* **12** 52
48. Lipstman I, Maniappan S and Goldberg I 2008 *Cryst. Growth Des.* **8** 1682
49. Wang K, Feng D, Liu T F, Su J, Yuan S, Chen Y P, Bosch M, Zou X and Zhou H C 2014 *J. Am. Chem. Soc.* **136** 13983
50. Alkordi M H, Liu Y, Larsen R W, Eubank J F and Eddaoudi M 2008 *J. Am. Chem. Soc.* **130** 12639
51. Bhyrappa P, Wilson S R and Suslick K S 1997 *J. Am. Chem. Soc.* **119** 8492
52. Bhyrappa P, Velkannan V and Varghese B 2008 *Acta Cryst* **E64** o190
53. Chen W, El-Khouly M E and Fukuzumi S 2011 *Inorg. Chem.* **50** 671
54. Krupitsky H, Zafra S, Goldberg I and Strouse C E 1994 *J. Inclu. Phenom. Mol. Recogn.* **18** 177
55. Bhyrappa P and Karunanithi K 2011 *Inorg. Chim. Acta* **372** 417
56. Lindsey J S and Wagner R W 1989 *J. Org. Chem.* **54** 828
57. Tamiaki H, Matsumoto N, Unno S, Shinoda S and Tsukube H 2000 *Inorg. Chim. Acta* **300** 243
58. Bhyrappa P and Krishnan V 1991 *Inorg. Chem.* **30** 239
59. Altomare A G, Cascarano G, Giacovazzo C and Gualardi A 1993 *J. Appl. Crystallogr.* **26** 343
60. Sheldrick G M 2008 *Acta Crystallogr.* **64A** 112
61. Farrugia L J 1997 *J. Appl. Crystallogr.* **30** 565
62. Bruno I J, Cole J C, Edgington P R, Kessler M, Macrae C F, McCabe P, Pearson J and Taylor J 2002 *Acta Crystallogr.* **B58** 389
63. Gouterman M 1978 In *The Porphyrins* Dolphin D (Eds.) (New York: Academic Press) Vol. 3 Ch 1
64. Sheer H, Katz J 1975 In *Porphyrins and Metalloporphyrins* Smith K M (Eds.) (New York: Elsevier) p. 399
65. Silvers S J and Tulinsky A 1967 *J. Am. Chem. Soc.* **89** 3331
66. Soman S, Sujatha S and Arunkumar C 2014 *J. Fluor. Chem.* **163** 16
67. Fleischer E B 1963 *J. Am. Chem. Soc.* **85** 1353
68. Chang C J, Deng Y, Heyduk A F, Chang C K and Nocera D G 2000 *Inorg. Chem.* **39** 959
69. Ehlinger N and Scheidt W R 1999 *Inorg. Chem.* **38** 1316
70. Hoard J L 1975 In *Porphyrins and Metalloporphyrins*, Smith K M (Eds.) (New York: Elsevier) p. 317
71. Scheidt W R, Mondal J U, Eigenbrot C W, Adler A, Radonovich L J and Hoard J L 1986 *Inorg. Chem.* **25** 795
72. Bhyrappa P Vaijayanthimala G and Varghese B 2002 *Tetrahedron Lett.* **43** 6427
73. Kim Y, Nam W, Lim M H, Jin S W, Lough A J and Kim S J 2001 *Acta Cryst.* **C51** 556
74. Desiraju G R and Parthasarathy R 1989 *J. Am. Chem. Soc.* **111** 8725
75. Desiraju G R, Steiner T 1999 *The weak hydrogen-bonding in structural chemistry and Biology.* IUCr monographs on Crystallography (UK: Oxford University Press) p. 215
76. Prasanna M D and Row T N 2000 *Cryst. Engg.* **3** 135
77. Sun L, Jentzen W, Shelnutt J A The Normal Coordinate Structural Decomposition Engine. http://jasheln.unm.edu/jasheln/content/nsd/NSDengine
78. Jentzen W, Ma J M and Shelnutt J A 1998 *Biophys. J.* **74** 753